Articles

Contribution from the Instituto de Desarrollo Tecnológico para la Industria Química (CONICET-UNL), Güemes 3450, 3000 Santa Fe, Argentina, Instituto de Física e Química de São Carlos, Universidade de São Paulo, C.P. 369, 13.560 São Carlos, SP, Brazil, and Departamento de Física, Facultad de Ciencias Exactas, Universidad Nacional de la Plata, C.C. 67, 1900 La Plata, Argentina

Molecular Structure and Exchange Interactions in *trans*-Bis(L-2-aminobutyrato)copper(II) and *trans*-Bis(D,L-2-aminobutyrato)copper(II)

P. R. Levstein,[†] R. Calvo,*[,†] E. E. Castellano,[‡] O. E. Piro,[§] and B. E. Rivero[§]

Received August 28, 1989

We examine the role of the lattice symmetry in the electronic paths for superexchange interactions in copper–amino acid complexes. For this purpose we obtained by ESR spectroscopy the exchange-coupling parameters J between coppers in *trans*-bis(L-2-aminobutyrato)copper(II), Cu(L-but)$_2$, and in *trans*-bis(D,L-2-aminobutyrato)copper(II), Cu(D,L-but)$_2$. Also, we solved the structure of Cu(L-but)$_2$, Cu($CO_2CH(NH_2)CH_2CH_3$)$_2$, and compared it with that reported by others for racemic Cu(D,L-but)$_2$. Cu(L-but)$_2$ crystallizes in the monoclinic space group $P2_1$ with a = 9.464 (3) Å, b = 5.060 (2) Å, c = 11.189 (4) Å, β = 90.60 (3)°, V = 535.8 (6) Å^3, Z = 2, D_{calc} = 1.664 g cm^{-3}, μ(Mo Kα) = 2.04 mm^{-1}, and F(000) = 278 electrons. The structure was solved by employing 1606 independent reflections with $I > 3\sigma(I)$ by Patterson and difference Fourier techniques and refined by full-matrix least squares to an agreement factor R = 0.06. The complex consists of Cu(II) ions in a square-planar trans coordination with N_2O_2 ligand sets, arranged in two-dimensional sheets parallel to (001). A pair of carboxylate oxygens from neighboring molecules in the sheet complete an elongated octahedral coordination around copper. The crystal is essentially isomorphous to the related Cu(D,L-but)$_2$ complex (space group $P2_1/c$), where Cu(II) ion is at a crystallographic inversion center. ESR measurements in Cu(L-but)$_2$ and Cu(D,L-but)$_2$ single crystals were performed at 34.1 GHz and room temperature. In each sample only one ESR exchange-collapsed line was observed for the two magnetically inequivalent copper ions in the lattice. The angular variations of its position and line width were measured in three perpendicular planes. The molecular gyromagnetic tensors of Cu(L-but)$_2$ and Cu(D,L-but)$_2$ obtained from these data are essentially equal, reflecting that the copper coordination and the relative orientation of the molecules in the crystal are very similar in the two systems. The values $g_\parallel$ = 2.257 (2.257) and $g_\perp$ = 2.056 (2.054) obtained for Cu(L-but)$_2$ (Cu(D,L-but)$_2$) indicate that the unpaired electron occupies the $d_{x^2-y^2}$ orbital. In the analysis of the ESR line width we use a model that considers the effect of the difference between the Zeeman interaction for the two rotated crystal sites for Cu(II). This model and our data allow us to obtain lower limits $|J| \geq 0.36$ K and $|J| \geq 0.59$ K for the isotropic exchange-coupling constants between inequivalent coppers in the Cu(L-but)$_2$ and Cu(D,L-but)$_2$ lattices, respectively. The large difference between the ESR line widths observed in Cu(L-but)$_2$ and Cu(D,L-but)$_2$ is interpreted as a result of the modification in the exchange network due to the descent in symmetry from Cu(D,L-but)$_2$ to Cu(L-but)$_2$, where the copper ions are not at inversion centers.

Introduction

Metal–amino acid complexes are good model systems to study electronic properties and exchange interactions between metal ions in proteinlike structures. From the biochemical point of view, it is important to correlate the magnitudes of the exchange interactions J between metal ions in these compounds with the chemical pathways connecting them. Also, the value of the isotropic exchange-coupling constant has been related to the rate constant of electron-transfer reactions in cases where the donor and acceptor molecules contain unpaired electrons.[1] In this scheme, magneto-structural correlations would lead, in a crude approximation, to kinetic-structural correlations in biological systems. It is then important to evaluate the exchange-coupling constants in compounds with known structures. The magnitudes of the exchange interaction J between nearest-neighbor copper ions in copper amino acid complexes, Cu(aa)$_2$, are of the order of tenths of a Kelvin degree, similar to the Zeeman energies involved in ESR measurements.[2-5] This fact, together with the existence of magnetically inequivalent ions in the lattice and various chemical paths between the paramagnetic ions, makes ESR spectroscopy the best suited technique to evaluate the absolute value of J in these systems. Exchange interactions with these magnitudes can be evaluated from room-temperature ESR data, while for magnetic susceptibility measurements very low temperatures would be required. Besides, in lattices with inequivalent sites for the metal ions, susceptibility data yield a mean value of the exchange interactions between magnetically equivalent and nonequivalent paramagnetic ions, while ESR data allow one to evaluate separately the J value between nonequivalent copper ions and to correlate it with the specific pathways between them.

In previous work, the X-band ESR study of a single crystal of bis(D,L-2-aminobutyrato)copper(II), Cu(D,L-but)$_2$, reflecting its magnetic layered structure was reported.[6] In this work, we perform the Q-band ESR study of the copper complexes of L-2-aminobutyric acid and of the racemic mixture D,L-2-aminobutyric acid. The similarities and the differences between the Q-band ESR data of these two structurally related systems give important clues about the exchange interactions.

In order to make magneto-structural correlations, the crystal structure of bis(L-2-aminobutyrato)copper(II), abbreviated Cu(L-but)$_2$, has been determined and is reported here. The structure of Cu(D,L-but)$_2$ has been reported by Fawcett et al.[7]

The ESR line width data at Q-band allow an evaluation of the exchange-coupling constant between nonequivalent coppers in both complexes using a model[4] that considers the rotation of the gy-

[†] Instituto de Desarrollo Tecnológico para la Industria Química (INTEC).
[‡] Universidade de São Paulo.
§ Universidad Nacional de la Plata.

(1) Okamura, M. Y.; Fredkin, D. R.; Isaacson, R. A.; Feher, G. In *Tunneling in Biological Systems*; Chance, et al., Eds.; Academic Press: New York, 1979; p 729.
(2) Newman, P. R.; Imes, J. L.; Cowen, J. A. *Phys. Rev. B* **1976**, *13*, 4093.
(3) Calvo, R.; Mesa, M. A.; Oliva, G.; Zukerman-Schpector, J.; Nascimento, O. R.; Tovar, M.; Arce, R. *J. Chem. Phys.* **1984**, *81*, 4584.
(4) Levstein, P. R.; Steren, C. A.; Gennaro, A. M.; Calvo, R. *Chem. Phys.* **1988**, *120*, 449.
(5) Steren, C. A.; Gennaro, A. M.; Levstein, P. R.; Calvo, R. *J. Phys.; Condens. Matter* **1989**, *1*, 637.
(6) Calvo, R.; Mesa, M. A. *Phys. Rev. B* 1983, *28*, 1244.
(7) Fawcett, T. G.; Ushay, M.; Rose, J. P.; Lalancette, R. A.; Potenza, J. A.; Schugar, H. J. *Inorg. Chem.* **1979**, *18*, 327. For comparison with our results, the $\hat{a}$ and $\hat{c}$ axes reported in this reference should be interchanged. An earlier two-dimensional X-ray study of Cu(D,L-but)$_2$ was reported by: Stosick, A. J. *J. Am. Chem. Soc.* **1945**, *67*, 362.

0020-1669/90/1329-3918$02.50/0

Table I. Crystallographic Data for Cu(L-but)$_2$

$Cu(H_2NCH(CO_2)CH_2CH_3)_2$	fw: 267.79
a = 9.464 (3) Å	T = 22 °C
b = 5.060 (2) Å	λ = 0.71073 Å
c = 11.189 (4) Å	ρ_{calcd} = 1.664 g cm^{-3}
β = 90.60 (3)°	μ = 20.4 cm^{-1}
V = 535.8 (6) Å^3	$F(000)$ = 278
Z = 2	R = 0.06
space group $P2_1$ (No. 4)	R_w = 0.063

romagnetic tensors for the two crystallographic sites for copper. The large differences between the line widths observed for the two complexes reflect important modifications of the exchange network, produced by the structural changes and the loss of symmetry from Cu(D,L-but)$_2$ to Cu(L-but)$_2$.

Experimental Section

Preparation of the Samples. The Cu(II) complexes of L-2-aminobutyric acid and D,L-2-aminobutyric acid were prepared by the urea hydrolysis technique.[7] In a typical experiment, 5.0 mmol of $CuCl_2 \cdot 2H_2O$ obtained from Merck and 10.0 mmol of L-2-aminobutyric acid (or D,L-2-aminobutyric acid) and 5.0 mmol of urea, obtained from Sigma, were dissolved in 80 mL of water. The solution was filtered through a Sartorius membrane (0.2-μm pore size) and maintained at 75 °C for 96 h. Both complexes crystallized as six-sided blue plates, and the crystals were separated from the hot solution by filtration, washed with water, and air-dried.

X-ray Diffraction Data. A complete X-ray diffraction data set was obtained at room temperature from a blue Cu(L-but)$_2$ crystal plate of dimensions 0.5 × 0.2 × 0.05 mm by employing an Enraf-Nonius CAD-4 four-circle diffractometer used with graphite-monochromated Mo Kα radiation. Unit cell parameters and the orientation matrix for data collection were obtained from 25 centered reflections in the range 13° < θ < 21°. Intensities were measured out to θ_{max} = 25° by using the ω–2θ scan mode. Scan rates were based on a prescan at 20° min^{-1} selected to give $I/\sigma(I) > 10$ with a maximum scan time of 20 s. X-ray background intensities were obtained by extending the scan 25% on both sides of the diffraction peak. Standard deviations of reflection intensities were calculated from counting statistics. The intensity of one standard reflection, monitored every 1800 s, was essentially constant during data collection period. Data were corrected for Lorentz, polarization, and absorption effects. An empirical absorption correction was applied by using the program DIFABS;[8] correction factors were in the 0.46–1.40 range. From 1869 independent reflections measured in the ±h,k,l reciprocal space quadrant, 1606 reflections having $I > 3\sigma(I)$ were used in the structure determination and refinement.

Bonded H atom scattering factors of Stewart et al.[9] and atomic scattering factors of Cromer and Waber and anomalous dispersion coefficients of Cromer and Ibers[10] for the rest of the atoms were used in the calculations. These were carried out on a VAX 730 computer with the SHELX[11] and SDP[12] systems of programs. The stereoscopic projections shown were drawn with the program ORTEP.[13]

Crystal Structure Determination and Refinement. The pertinent crystallographic data for Cu(L-but)$_2$ are given in Table I. The structure was solved by standard Patterson and difference Fourier techniques. Non-hydrogen atoms were refined with anisotropic thermal parameters. All but the methyl hydrogen atoms were located from difference Fourier maps and included in the structure factor calculaton with a common fixed temperature parameter B = 3.95 Å^2. In the final cycle of full-matrix least-squares refinement, employing the minimization function $M = \sum w(|F_o| - |F_c|)^2$ with weights $w = [\sigma^2(|F_o|) + 0.002|F_o|^2]^{-1}$, the shifts of the parameters were within 0.05 times their standard deviation. The corresponding final difference Fourier map showed minimum and maximum values of −1.5 and 2.6 e Å^{-3} located close to the copper ion. Final agreement factors, defined as $R = (\sum||F_o| - |F_c||)/\sum|F_o|$ and $R_w = [\sum w(|F_o| - |F_c|)^2/\sum w|F_o|^2]^{1/2}$ are given in Table I. A crystallographic test of chirality performed at this stage confirmed the L form of the aminobutyric acid molecules in the crystal. A list of observed and calculated structure factor amplitudes is available as supplementary material.

Table II. Fractional Atomic Coordinates and Isotropic Temperature Factors (Å^2) for Bis(L-2-aminobutyrato)copper(II)

atom	x/a	y/b	z/c	B_{iso}
Cu	0.7523 (1)	0	0.0106 (1)	1.76 (3)
O(11)	0.9169 (4)	−0.211 (1)	−0.0351 (4)	1.6 (1)
O(12)	1.0951 (5)	−0.207 (1)	−0.1635 (5)	2.2 (2)
N(1)	0.8173 (6)	0.239 (1)	−0.1187 (5)	1.7 (2)
C(11)	0.9785 (7)	−0.127 (1)	−0.1278 (6)	1.6 (2)
C(12)	0.8918 (6)	0.070 (1)	−0.2042 (6)	1.6 (2)
C(13)	0.9766 (8)	0.222 (2)	−0.2970 (7)	2.5 (2)
C(14)	0.880 (1)	0.375 (2)	−0.3840 (9)	4.5 (4)
O(21)	0.5860 (5)	0.208 (1)	0.0523 (5)	1.8 (2)
O(22)	0.3906 (5)	0.197 (1)	0.1594 (5)	2.4 (2)
N(2)	0.6775 (5)	−0.258 (1)	0.1282 (5)	1.6 (2)
C(21)	0.5086 (7)	0.110 (1)	0.1315 (6)	1.5 (2)
C(22)	0.5623 (7)	−0.136 (2)	0.1987 (7)	1.6 (2)
C(23)	0.615 (1)	−0.050 (2)	0.3232 (6)	3.0 (3)
C(24)	0.641 (1)	−0.289 (2)	0.4070 (9)	4.4 (4)

Table III. Bond Distances (Å) and Angles (deg) for Cu(L-but)$_2$

(a) Bond Distances

Cu–O(11)	1.962 (4)	Cu–O(21)	1.955 (5)
Cu–N(1)	1.985 (6)	Cu–N(2)	1.986 (6)
Cu–O(12′)[a]	2.679 (5)	Cu–O(22′)[b]	2.787 (5)
O(11)–C(11)	1.267 (8)	O(21)–C(21)	1.256 (8)
C(11)–O(12)	1.246 (8)	C(21)–O(22)	1.244 (8)
C(11)–C(12)	1.54 (1)	C(21)–C(22)	1.54 (1)
C(12)–N(1)	1.471 (9)	C(22)–N(2)	1.488 (9)
C(12)–C(13)	1.52 (1)	C(22)–C(23)	1.54 (1)
C(13)–C(14)	1.54 (1)	C(23)–C(24)	1.55 (1)

(b) Bond Angles

N(1)–Cu–O(11)	83.6 (2)	N(2)–Cu–O(21)	84.4 (2)
N(1)–Cu–N(2)	174.6 (2)	O(11)–Cu–O(21)	178.6 (2)
N(1)–Cu–O(21)	95.9 (2)	N(2)–Cu–O(11)	96.0 (2)
O(12′)[a]–Cu–N(1)	87.7 (2)	O(12′)[a]–Cu–N(2)	97.7 (2)
O(12′)[a]–Cu–O(11)	92.6 (2)	O(12′)[a]–Cu–O(21)	88.7 (2)
O(22′)[b]–Cu–N(1)	89.4 (2)	O(22′)[b]–Cu–N(2)	85.2 (2)
O(22′)[b]–Cu–O(11)	84.4 (2)	O(22′)[b]–Cu–O(21)	94.3 (2)
Cu–O(11)–C(11)	113.9 (4)	Cu–O(21)–C(21)	115.7 (4)
Cu–N(1)–C(12)	105.9 (4)	Cu–N(2)–C(22)	110.3 (4)
O(11)–Cu(11)–O(12)	124.8 (6)	O(21)–C(21)–O(22)	124.7 (6)
O(11)–C(11)–C(12)	114.9 (6)	O(21)–C(21)–C(22)	118.0 (6)
O(12)–C(11)–C(12)	120.0 (6)	O(22)–C(21)–C(22)	117.2 (6)
N(1)–C(12)–C(11)	105.8 (5)	N(2)–C(22)–C(21)	108.6 (6)
N(1)–C(12)–C(13)	114.1 (6)	N(2)–C(22)–C(23)	111.5 (6)
C(11)–C(12)–C(13)	114.8 (6)	C(21)–C(22)–C(23)	108.3 (6)
C(12)–C(13)–C(14)	111.7 (7)	C(22)–C(23)–C(24)	112.0 (7)
O(12′)[a]–Cu–O(22′)[b]	176.0 (2)		

[a] The symmetry operation 2 − x, y + $^1/_2$, z transforms O(12) into O(12′). [b] The symmetry operation 1 − x, y − $^1/_2$, z transforms O(22) into O(22′).

EPR Measurements. Single crystals of Cu(L-but)$_2$ and Cu(D,L-but)$_2$ with sizes about 2.5 × 1.2 × 0.1 mm were glued to respective sample holders with the $\hat{a}$, $\hat{b}$, and $\hat{c}' = \hat{a} \times \hat{b}$ axes of the Cu(L-but)$_2$ specimen and the $\hat{c}$, $\hat{b}$, and $\hat{a}' = \hat{b} \times \hat{c}$ axes of the Cu(D,L-but)$_2$ sample along the $\hat{x}$, $\hat{y}$, and $\hat{z}$ axes, respectively, of an orthogonal reference system defined with respect to the holder. The EPR measurements were performed at room temperature with an ER-200 Bruker spectrometer, a rotating 12-in. electromagnet with a Hall probe control, and a Bruker cylindrical cavity working at 34.1 GHz, with rotating 100-kHz modulation coils. The magnetic field was calibrated with DPPH. In each experiment, the sample holder was positioned in a pedestal having an horizontal plane inside the cavity, so that the applied magnetic field $\vec{B}$ could be accurately rotated in the xy, yz, or zx planes of the samples, and the spectra were recorded at intervals of 10°. The orientation of the magnetic field within the xy and zy planes was determined by using the ESR data and the known crystal symmetry. The orientation of the magnetic field in the zx plane was accurately defined by matching the angular variation of the spectra in this plane with those obtained in the other two planes.

Results and Discussion

Structural Results. Atomic fractional coordinates and equivalent isotropic temperature parameters calculated by following Ham-

(8) Walker, N.; Stuart, D. *Acta Crystallogr., Sect. A* **1983**, *A39*, 158.
(9) Stewart, R. F.; Davison, E. R.; Simpson, W. T. *J. Chem. Phys.* **1965**, *42*, 3175.
(10) Cromer, D. T.; Waber, J. T. *International Tables X-ray Crystallography*; Kynoch Press: Birmingham, England, 1974; Vol. IV, p 71. Cromer, D. T.; Ibers, J. A. IBID., p 149.
(11) Sheldrick, G. M. *SHELX, A Program for Crystal Structure Determinations*; University of Cambridge: Cambridge, England, 1976.
(12) Frenz, B. A. *Enraf-Nonius Structure Determination Package*; Enraf-Nonius: Delft, The Netherlands, 1983.
(13) Johnson, C. K. ORTEP; Report ORNL-3794; Oak Ridge National Laboratory: Oak Ridge, TN, 1965.

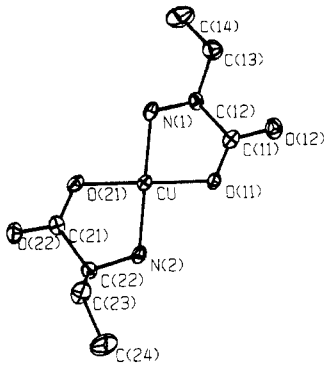

Figure 1. Molecular structure of the bis(L-2-aminobutyrato)copper(II) molecule, showing the labeling of atoms and their thermal vibration ellipsoids.

ilton[14] for Cu(L-but)$_2$ are given in Table II. Relevant interatomic bond distances and angles are in Table III. Figure 1 is a drawing of the copper–aminobutyric acid complex, showing the atom-numbering scheme. A stereoscopic view of the crystal packing is shown in Figure 2. Listings of anisotropic thermal parameters for the non-hydrogen atoms, coordinates of the determined hydrogen atoms, hydrogen-bond distances and angles, and the relevant least-squares planes and dihedral and torsional angles for the complex are provided as supplementary material.

Trans coordination of Cu(II) ion by two aminobutyric acid molecules produces an essentially planar (within ± 0.05 Å) CuN_2O_2 configuration (see Figures 1 and 2) with mean Cu–N and Cu–O bond distances of 1.959 (5) and 1.986 (6) Å, respectively. Additional interactions of copper with two carboxylate oxygen atoms from neighboring molecules (Cu–O bond lengths of 2.679 (5) and 2.787 (5) Å) complete an elongated octahedral environment around the metal ion (see Figure 2). The Cu(L-but)$_2$ complexes are arranged in two-dimensional sheets parallel to the *ab* plane. The molecules are linked to each other within the sheet through the intermolecular Cu–O interaction already mentioned and also through a net of relatively weak N–H···O hydrogen bonds (H···O distances larger than 2.23 Å). Neighboring sheets are held together by van der Waals interactions.

Cu(L-but)$_2$ is practically isomorphous to Cu(D,L-but)$_2$, which crystallizes in the centrosymmetric space group $P2_1/c$, with essentially the same cell constants.[7,15] In Cu(D,L-but)$_2$, the Cu(II) ion is located on a crystallographic inversion center that symmetry relates the pair of dextro and levo aminobutyric acid molecules bound to the copper ion. The coordination around this ion is completed with a symmetry-related pair of carboxylate oxygens from neighboring molecules [d(Cu–O) = 2.758 (3) Å]. As in the case of Cu(L-but)$_2$, Cu(D,L-but)$_2$ presents carboxylate-bridged sheets of Cu(II) ions with further links between Cu(D,L-but)$_2$ units within a sheet due to relatively weak N–H···O hydrogen bonds.

The atomic coordinates obtained for Cu(L-but)$_2$ hold a close relationship with those for centrosymmetric Cu(D,L-but)$_2$ for all but the side group atoms of corresponding L and D aminobutyric acid molecules in the respective complexes.[15] The isomorphism around copper is slightly disrupted mainly due to a small asymmetry in the apical Cu–O distances (of about 0.1 Å) and to a slight deviation (of about 4°) in the axial O–Cu–O angle from 180° exhibited by Cu(L-but)$_2$ compared with the perfect centrosymmetric environment of copper in Cu(D,L-but)$_2$.

ESR Results. Gyromagnetic Factor. In Cu(L-but)$_2$ and Cu(D,L-but)$_2$, a single exchange-collapsed ESR line was observed for the two magnetically inequivalent copper ions, for any orientation $\hat{h} = \vec{B}/|\vec{B}| = (\sin\theta\cos\phi, \sin\theta\sin\phi, \cos\theta)$ of the applied field $\vec{B}$. The experimental values for the squared gyromagnetic factors $g^2(\theta,\phi)$ are displayed in Figures 3 and 4. The observed positions of the ESR lines were fitted to an effective spin Hamiltonian

$$\mathcal{H} = \mu_B \vec{B}\cdot\mathbf{g}\cdot\vec{S} \qquad (1)$$

where μ_B is the Bohr magneton, $\mathbf{g} = (\mathbf{g}_A + \mathbf{g}_B)/2$ the gyromagnetic tensor, and $\vec{S}$ the effective spin operator ($S = {}^1/_2$). In each case, the values measured for $g^2(\theta,\phi) = \hat{h}\cdot\mathbf{g}\cdot\mathbf{g}\cdot\hat{h}$ were used to evaluate the tensor g^2 by a least-squares method and the components of $\mathbf{g}^2$ are included in Table IV. The solid lines in Figures 3 and 4 were calculated with these tensors. From crystallographic data, we may assume axial symmetry for the molecular gyromagnetic tensors $\mathbf{g}_A$ and $\mathbf{g}_B$ corresponding to copper in the symmetry-related sites A and B, with $g_\perp$ in the plane of ligands and $g_\parallel$ perpendicular to it. Then, we calculated $g_\perp$, $g_\parallel$, the orientation (θ_m,ϕ_m) of the molecular axis of one site, and the angle 2α between the axes of the two copper sites, using our experimental data in each complex and the method of Abe and Ono,[16] detailed in ref 6. These values are given in Table IV along with related crystallographic information. It can be appreciated from this table that the molecular orientations (θ_m,ϕ_m) and 2α calculated from the ESR data agree well with the corresponding orientations obtained from X-ray diffraction data.

Table IV. Values of the Components of the $\mathbf{g}^2$ Tensors Obtained by Least-Squares Analyses of the Data Taken at 34.1 GHz[a]

	Cu(L-but)$_2$	Cu(D,L-but)$_2$
$(g^2)_{xx}$	4.5035 ± 0.0007	4.4688 ± 0.0006
$(g^2)_{yy}$	4.4372 ± 0.0007	4.4180 ± 0.0006
$(g^2)_{zz}$	4.6051 ± 0.0007	4.6456 ± 0.0006
$(g^2)_{xz}$	0.3239 ± 0.0009	0.3255 ± 0.0007
$(g^2)_{xy}$	0.0000 ± 0.0009	0.0000 ± 0.0007
$(g^2)_{yz}$	0.0000 ± 0.0009	0.0000 ± 0.0007
$(g^2)_1$	4.882 ± 0.001	4.8945 ± 0.0008
$(g^2)_2$	4.226 ± 0.001	4.2199 ± 0.0008
$(g^2)_3$	4.4372 ± 0.0008	4.4180 ± 0.0006
$\hat{a}_1$	(0.76,0,–0.65)	(0.794,0,–0.607)
$\hat{a}_2$	(0.65,0,0.76)	(0.607,0,0.794)
$\hat{a}_3$	(0,–1,0)	(0,1,0)
$g_\parallel$	2.257 ± 0.001	2.257 ± 0.001
$g_\perp$	2.056 ± 0.001	2.054 ± 0.001
θ_m, deg	48.6 (45.8)	45.7 (44.6)
ϕ_m, deg	138.9 (138.5)	138.3 (140.1)
2α, deg	120.9 (123.2)	123.1 (126.5)

[a] $(g^2)_1$, $(g^2)_2$, and $(g^2)_3$ and $\hat{a}_1$, $\hat{a}_2$, and $\hat{a}_3$ are the eigenvalues and eigenvectors of the $\mathbf{g}^2$ tensors in the coordinate systems $xyz = abc'$ for Cu(L-but)$_2$ and $xyz = cba'$ for Cu(D,L-but)$_2$.

ESR Results. Line Width Data. Line width data obtained for Cu(D,L-but)$_2$ and Cu(L-but)$_2$ are displayed in Figure 5. Several sources of line broadening and narrowing of the ESR signal are present in pure metal–amino acid complexes.[4,5,17] In this work we are specifically interested in the evaluation of the exchange-coupling constant J' between magnetically nonequivalent copper ions linked by carboxylate bridges. In these systems, the exchange Hamiltonian can be written as

$$\mathcal{H}_{ex} = {}^1/_2\sum_{ij}{}' J_{ij}^{AA}\vec{S}_i^A\cdot\vec{S}_j^A + {}^1/_2\sum_{ij}{}' J_{ij}^{BB}\vec{S}_i^B\cdot\vec{S}_j^B + \sum_{ij} J_{ij}^{AB}\vec{S}_i^A\cdot\vec{S}_j^B \qquad (2)$$

where A and B denote the two symmetry-related copper sites, which are magnetically inequivalent for an arbitrary orientation of the applied field $\vec{B}$, and i and j indicate different unit cell. For the present purpose J_{ij} will be restricted to a nearest-neighbor interaction with $J_{ij}^{AA} = J_{ij}^{BB} = J$ and $J_{ij}^{AB} = J'$. In order to

(14) Hamilton, W. C. *Acta Crystallogr.* **1959**, *12*, 609.
(15) The values of the parameters a, b, and c determined in this work for Cu(L-but)$_2$ should be compared to those of c, b, and a determined in ref 7 for Cu(D,L-but)$_2$. Besides, the atomic fractional coordinates (x_L, y_L, z_L) of Cu(L-but)$_2$ in Table II are approximately related to the corresponding atom positions (x_{DL}, y_{DL}, z_{DL}) of the quasi-isomorphous Cu(D,L-but)$_2$ crystal reported in ref 7 through $x_L = z_{DL} + {}^3/_4$, $y_L = y_{DL}$ $- {}^1/_2$, and $z_L = -x_{DL}$.
(16) Abe, H.; Ono, K. *J. Phys. Soc. Jpn.* **1956**, *11*, 947.
(17) Gennaro, A. M.; Levstein P. R.; Steren, C. A.; Calvo, R. *Chem. Phys.* **1987**, *111*, 431.

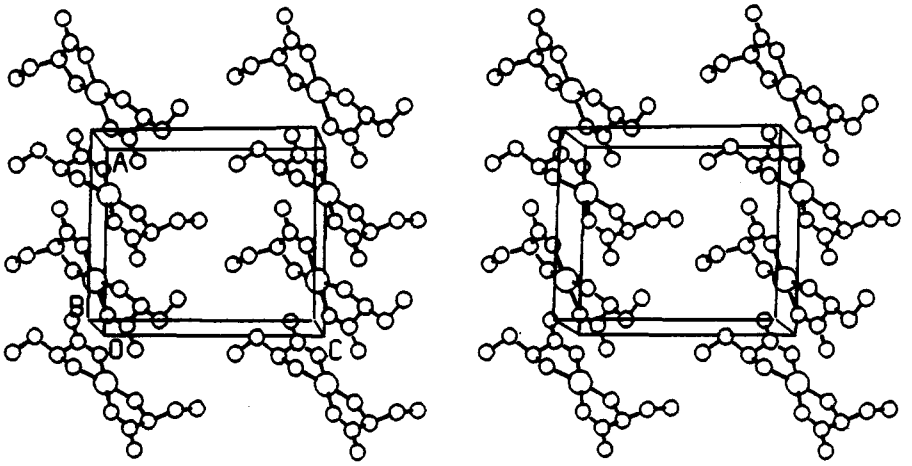

Figure 2. Stereoscopic projection of the Cu(L-but)$_2$ crystal viewed along $\hat{b}$. The $\hat{a}$ axis is horizontal.

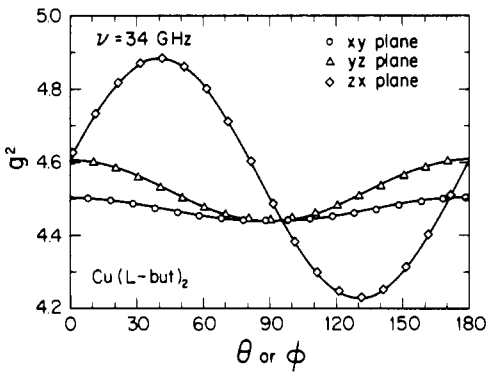

Figure 3. Angular variation of the squared gyromagnetic factor measured at 300 K and 34.1 GHz in three orthogonal planes of a Cu(L-but)$_2$ single crystal. The curves were obtained by fitting the data with a symmetric $\mathbf{g}^2$ second-order tensor. The parameters of the fit are included in Table IV.

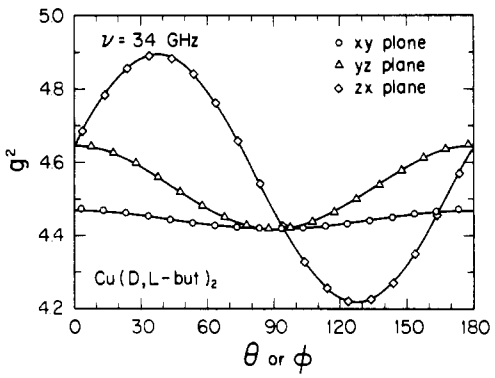

Figure 4. Angular variation of the squared gyromagnetic factor measured at 300 K and 34.1 GHz in three orthogonal planes of a Cu(D,L-but)$_2$ single crystal. The curves were obtained by fitting the data with a symmetric $\mathbf{g}^2$ second-order tensor. The parameters of the fit are included in the Table IV.

evaluate J', the experimental data for the peak-to-peak line width displayed in Figure 5 were fitted to the angular function

$$\Delta B(\theta,\phi) = A_1 \sin^2\theta\cos^2\phi + A_2 \sin^2\theta\sin^2\phi + A_3\cos^2\theta + A_4\, 2\sin\theta\cos\phi\cos\theta + A_5[g_A(\theta,\phi) - g_B(\theta,\phi)]^2 + A_6\cos^4\theta \quad (3)$$

The angular functions mutiplying the coefficients A_1–A_4 in eq 3 are proportional to second-order spherical harmonics and can be separated from the two last terms, which contain fourth-order spherical harmonics.

The solid lines in Figure 5 were obtained from the respective fits, and the A_i coefficients are shown in Table V. The terms of eq 3 corresponding to the A_i values, with $i \neq 5$, consider the magnetic dipolar, hyperfine, and antisymmetric exchange contributions to the line width.[17,18] They do not interfere with the angular variation of the residual Zeeman contribution arising from the existence of two magnetically inequivalent copper ions in the lattice, characterized by the A_5 contribution. The term involving

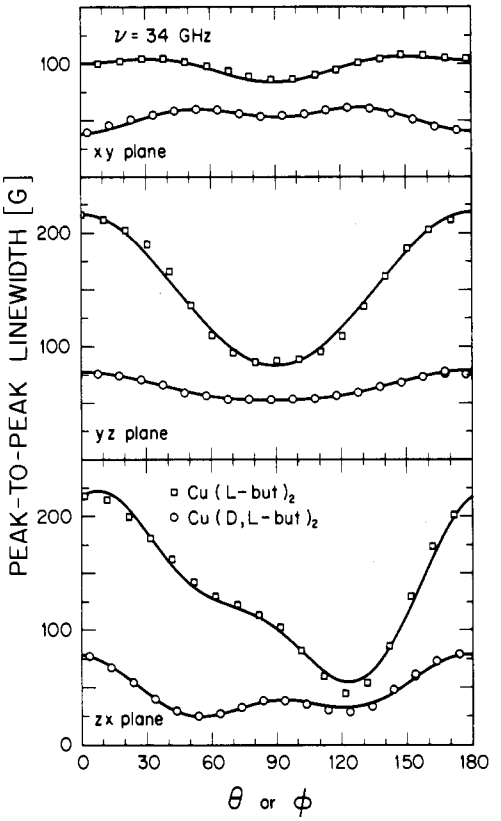

Figure 5. Angular variations of the peak-to-peak line width measured at 300 K and 34.1 GHz in the three principal planes of Cu(L-but)$_2$ and Cu(D,L-but)$_2$ single crystals. The curves were obtained from least-squares fits of the line width data to eq 3. The parameters from these fits are given in Table V.

Table V. Values of the Coefficients Obtained by Least-Squares Fits of Eq 3 to the Line Width Data Taken at 34.1 GHz and at 300 K, Displayed in Figure 5

	Cu(L-but)$_2$	Cu(D,L-but)$_2$		Cu(L-but)$_2$	Cu(D,L-but)$_2$
A_1	93 ± 2	38.6 ± 0.4	A_4	42 ± 2	4.0 ± 0.5
A_2	80 ± 2	52.3 ± 0.6	A_5	1956 ± 170	1195 ± 43
A_3	55 ± 9	27 ± 2	A_6	162 ± 10	105 ± 3

(18) Soos, Z. G.; McGregor, K. T.; Cheung, T. T. P.; Silverstein, A. J. *Phys. Rev. B* **1977**, *16*, 3036.

A_6 considers the broadening produced by the dipole–dipole interaction in a lattice made of copper layers parallel to the *ab* plane.

As it was explained in a previous paper,[4] the A_5 coefficient can be calculated by using the Kubo and Tomita formalism[19] and results as

$$A_5 = \frac{\nu^2 h^2 \sqrt{2\pi/3}}{8|J'|\mu_B g^3} \quad (4)$$

where h is the Planck constant, ν is the Larmor frequency, and g is the mean gyromagnetic factor. The values of A_5 are negligible in ESR experiments performed at X-band (9.7 GHz). Equation 4 and the results of the fits allow us to obtain the values $|J'| = 0.36 \pm 0.03$ K for Cu(L-but)$_2$ and $|J'| = 0.59 \pm 0.02$ K for Cu(D,L-but)$_2$. They must be taken as lower limits of $|J'|$ because the model[4] neglects the effects on the spin dynamics of the low magnetic dimensionality of these systems.[20] However, comparisons between values calculated by this method with those obtained from susceptibility measurements[2,3] indicate that the method provides very reliable values. The assumptions made in the evaluation of $|J'|$ deserve another comment. In eq 4, $|J'|$ is the mean exchange-coupling constant between neighboring inequivalent copper ions. This value coincides strictly with the value of the exchange constant between pairs of nonequivalent copper neighbors in Cu(D,L-but)$_2$ because each copper ion has four magnetically inequivalent copper neighbors linked by exactly the same pathways. This is not true for Cu(L-but)$_2$, where the copper ions are not at inversion centers and each copper has four magnetically inequivalent copper neighbors with pathways equal by pairs. Then

$$|J'| = \frac{\sqrt{z_1 J_1^2 + z_2 J_2^2}}{z_1 + z_2} \quad (5)$$

where z_1 and z_2 are the number of nearest neighbors linked by connections J_1 and J_2, respectively. In this case, if we assume that the asymmetry may lead to the neglect of J_2, then J_1 would reach a value of 0.51 K. This assumption is supported in a previously observed correlation between the $|J'|$ values and the copper–apical oxygen bond lengths (Cu–O_{ap}), which indicate that $|J'|$ decreases for larger values of the Cu–O_{ap} distances,[21] and in the fact that in Cu(L-but)$_2$ the lengths of the Cu–O_{ap} bonds are 2.68 and 2.79 Å. The important consequence of this variation in the exchange network from Cu(D,L-but)$_2$ to Cu(L-but)$_2$ is the descent in the magnetic dimensionality. Thus, the time correlation functions, which for long times are governed by the spin diffusion, decay slower in Cu(L-but)$_2$ than in Cu(D,L-but)$_2$, producing a wider ESR line in the former. This fact can be observed in the experimental results displayed in Figure 5.

Conclusions

The structural results and the values $g_\parallel = 2.257$ (2.257) and $g_\perp = 2.056$ (2.054) obtained for the molecular gyromagnetic factors of Cu(II) in Cu(L-but)$_2$ and Cu(D,L-but)$_2$, respectively, reflect similarity of the local ligand field interaction acting on Cu(II) ions in Cu(L-but)$_2$ and Cu(D,L-but)$_2$. As can be inferred from the $g_\parallel$ and $g_\perp$ values, the unpaired electron occupies the $d_{x^2-y^2}$ orbital.[22] If we compare the two complexes, it can be seen in Table IV that the directions of the normals to the square of ligands to coppers calculated from ESR and crystallographic data differ only by about two degrees. Thus, even the relative orientations of the molecules in the crystals are very similar. However, as it is shown in Figure 5, the ESR peak-to-peak line widths present strong differences between the two complexes, and consequently different values of J' are obtained. The difference in the ESR line widths observed between Cu(L-but)$_2$ and Cu(D,L-but)$_2$ arises from two sources. First, the lengths of the two apical oxygen–copper bonds are different in Cu(L-but)$_2$ but equal by symmetry in Cu(D,L-but)$_2$; this difference is significant enough to modify the J' value.[21,23] Second, this change of the exchange-coupling constant produced by the variation in the structural parameters is amplified in the ESR line width due to the diffusive long-time behavior of the spin dynamics in magnetically low-dimensional systems.[20] In particular, the exchange network of Cu(D,L-but)$_2$ has two-dimensional characteristics, while in the L-compound there is a preferred direction for the exchange coupling. This produces a slower spin dynamics in Cu(L-but)$_2$ and consequently larger ESR line widths.[19,20]

Acknowledgment. This work was supported by the Consejo Nacional de Investigaciones Cientificas y Tecnicas (CONICET) of Argentina, through Grants PID 3-905608 and 3-907602/85, by the Fundacão de Amparo a Pesquisa do Estado de São Paulo, Brazil, and by Grant RG86-14 of the Third World Academy of Sciences. Support from the exchange program between CONICET and the Conselho Nacional de Desenvolvimento Cientifico e Tecnológico (Brazil) is also gratefully acknowledged.

Registry No. Cu(L-but)$_2$, 14407-52-4; Cu(D,L-but)$_2$, 10171-05-8.

Supplementary Material Available: Listings of anisotropic thermal parameters for the non-hydrogen atoms (Table VI), fractional coordinates of the determined hydrogen atoms (Table VII), hydrogen-bond distances and angles (Table VIII), and least-squares planes and dihedral and torsional angles for Cu(L-but)$_2$ (Table X) (4 pages); a listing of calculated and observed structure factor amplitudes with standard deviations (Table IX) (9 pages). Ordering information is given on any current masthead page.

(19) Kubo, R.; Tomita, K. *J. Phys. Soc. Jpn.* **1954**, *9*, 888.
(20) Richards, P. M. In *Local Properties at Phase Transitions*; Editrice Compositori: Bologna, Italy, 1975; p 539.
(21) Levstein, P. R.; Calvo, R. *Inorg. Chem.* **1990**, *29*, 1581.
(22) Zeiger, H. J.; Pratt, G. W. *Magnetic Interactions in Solids*; Oxford University Press: London, 1973.
(23) Hay, J. P.; Thibeault, J. C.; Hoffmann, R. *J. Am. Chem. Soc.* **1975**, *97*, 4884.